

**OAK RIDGE NATIONAL LABORATORY**

operated by

**UNION CARBIDE CORPORATION**

for the

**U.S. ATOMIC ENERGY COMMISSION**



ORNL-TM-339

*W. J.*  
*68*

EFFECT OF CO<sub>2</sub> ON THE STRENGTH AND DUCTILITY OF TYPE 304  
STAINLESS STEEL AT ELEVATED TEMPERATURES

W. R. Martin  
H. E. McCoy, Jr.

**NOTICE**

This document contains information of a preliminary nature and was prepared primarily for internal use at the Oak Ridge National Laboratory. It is subject to revision or correction and therefore does not represent a final report. The information is not to be abstracted, reprinted or otherwise given public dissemination without the approval of the ORNL patent branch, Legal and Information Control Department.

LEGAL NOTICE

This report was prepared as an account of Government sponsored work. Neither the United States, nor the Commission, nor any person acting on behalf of the Commission:

- A. Makes any warranty or representation, expressed or implied, with respect to the accuracy, completeness, or usefulness of the information contained in this report, or that the use of any information, apparatus, method, or process disclosed in this report may not infringe privately owned rights; or
- B. Assumes any liabilities with respect to the use of, or for damages resulting from the use of any information, apparatus, method, or process disclosed in this report.

As used in the above, "person acting on behalf of the Commission" includes any employee or contractor of the Commission, or employee of such contractor, to the extent that such employee or contractor of the Commission, or employee of such contractor prepares, disseminates, or provides access to, any information pursuant to his employment or contract with the Commission, or his employment with such contractor.

ORNL-TM-339

Copy

Contract No. W-7405-eng-26

METALS AND CERAMICS DIVISION

EFFECT OF CO<sub>2</sub> ON THE STRENGTH AND DUCTILITY OF TYPE 304  
STAINLESS STEEL AT ELEVATED TEMPERATURES

W. R. Martin and H. E. McCoy, Jr.

DATE ISSUED

**SEP 27 1962**

---

OAK RIDGE NATIONAL LABORATORY  
Oak Ridge, Tennessee  
operated by  
UNION CARBIDE CORPORATION  
for the  
U. S. ATOMIC ENERGY COMMISSION

## ABSTRACT

One of the important problems in determining the usefulness of stainless steels as cladding materials in high-temperature gas-cooled reactors is the effect that their reactions with the coolant has on their strength and ductility. The mechanisms by which the coolant ( $\text{CO}_2$  in this investigation) affects the strength properties of type 304 stainless steel are being investigated in the range 1300 to 1700°F (704–927°C). Creep- and stress-rupture results obtained on sheet materials in wet and dry  $\text{CO}_2$  and argon are compared. The effect of annealing in  $\text{CO}_2$  on the tensile strength and ductility was also investigated.

The question of whether the strengthening observed in  $\text{CO}_2$  was due to oxidation or carburization was investigated. Experiments on the effect of various partial pressures of oxygen in argon showed that the creep rate was minimum at approximately 10 ppm. The creep rate in  $\text{CO}_2$  at equivalent stress and temperature was lower by a factor of 3 than the minimum rate observed in oxygen. Chemical analyses, metallography, and experiments with  $\text{C}^{14}$  showed that carburization occurred in pure flowing  $\text{CO}_2$  in the temperature range studied. From this evidence it was concluded that the strengthening observed in  $\text{CO}_2$  was primarily due to carburization.

The creep- and tensile-fracture strains were adversely affected by exposure to  $\text{CO}_2$ , with the magnitude of the effect dependent on the time and temperature of exposure.

EFFECT OF CO<sub>2</sub> ON THE STRENGTH AND DUCTILITY OF TYPE 304  
STAINLESS STEEL AT ELEVATED TEMPERATURES

W. R. Martin and H. E. McCoy

INTRODUCTION

The application of engineering materials in the design of devices that operate at elevated temperatures requires a thorough knowledge of both the conditions under which the device operates and the resulting effect on the various component materials - for example, the fuel element cladding, which contains the reactor fuel and fission gases. Fuel element cladding materials must satisfy nuclear physics requirements and allow a fuel burnup consistent with economy.

In a gas-cooled reactor, interactions between the fuel cladding material and the coolant (or its impurities) may produce deleterious effects on the mechanical properties and thereby shorten the life of the fuel element.

Although other gases have been considered as coolants and other materials as fuel element claddings, the concern here is with CO<sub>2</sub> and type 304 stainless steel.

EXPERIMENTAL TECHNIQUES, EQUIPMENT, AND MATERIALS

The gaseous environment surrounding the specimen during creep rupture was controlled by means of a test chamber similar to that shown in Fig. 1. The test chamber is a type 310 stainless steel tube wrapped with a Nichrome wire heating element. The extension rod and the test chamber are joined with U-cup pressure-vacuum seals, which maintained vacuum or pressure within the test chamber without restricting the movement of the extension rods. The seals are cooled by water jackets placed at the top and at the bottom of the chamber. Four Chromel-Alumel thermocouples were inserted in the top of the chamber, two of them made with standard insulators and attached directly to the gage length of the specimen, and the other two were swaged assemblies

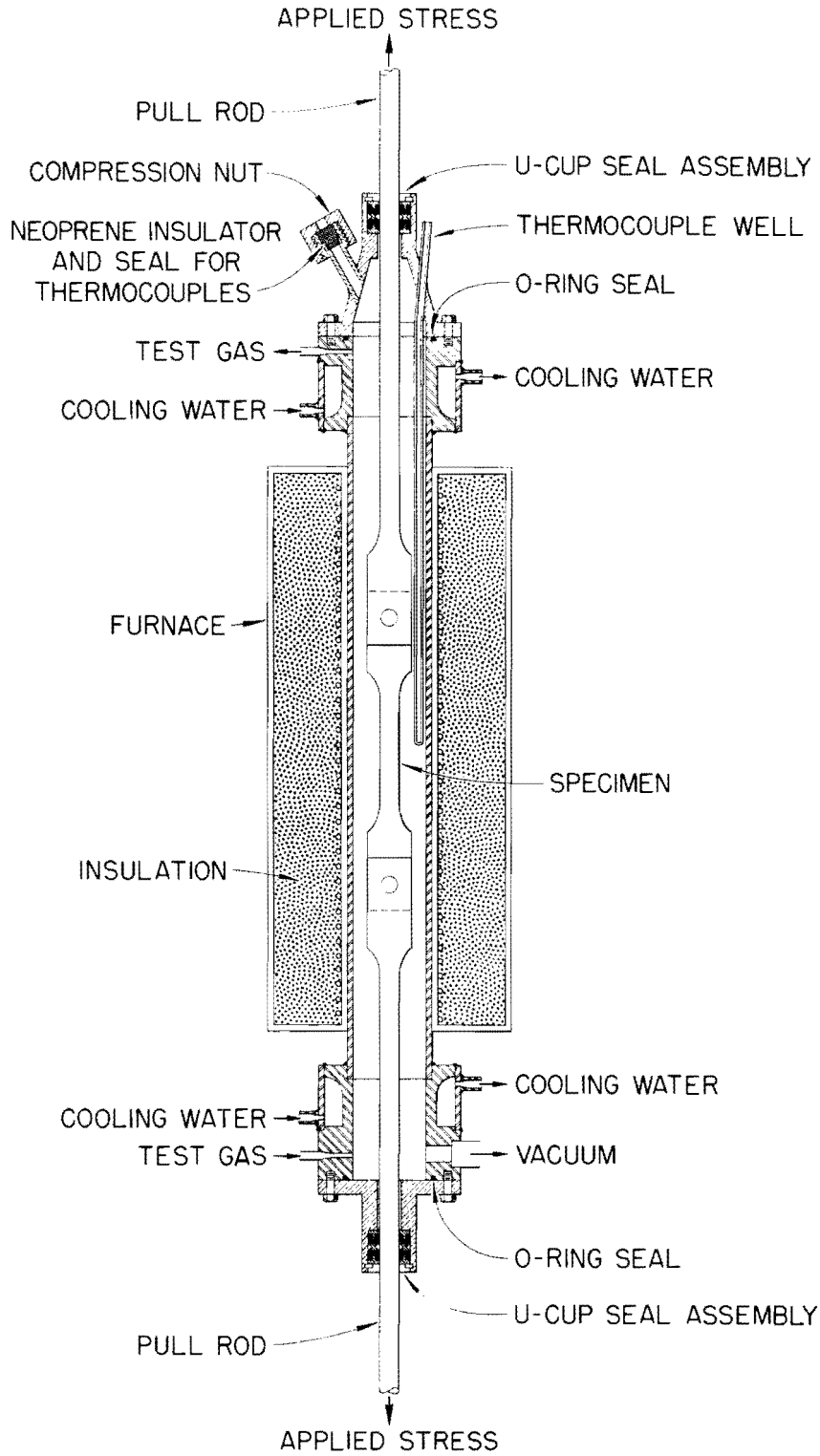


Fig. 1. Chamber for Environmental Stress-Rupture Tests at Elevated Temperatures.

consisting of Chromel-Alumel wires, magnesium oxide insulation, and Inconel sheathing. The elongation of the specimen was measured by a dial gage which indicated the movement of the external pull rod.

Stress-rupture tests were performed in controlled gaseous environments. After the system was checked for leaks to prevent contamination of the test environment, the CO<sub>2</sub> was introduced in one of two ways. In one method the CO<sub>2</sub> was introduced directly into the chamber and then the specimen was heated to test temperature. In the second method the specimen was heated to test temperature under a vacuum of less than 1  $\mu$  before the CO<sub>2</sub> was introduced, which minimized the length of time that the specimen was exposed to the test environment. Tests in gases that react chemically with the chamber were run in flowing environments, and those in argon, which was introduced by the second method, were run under static conditions. Although high-purity argon was used, zirconium strips were suspended near the specimen to act as a getter.

The initial temperature distribution across the test section of the specimen was determined by thermocouples attached to the specimen. Since CO<sub>2</sub> reacted with Chromel-Alumel thermocouples to alter their temperature-emf characteristics, swaged thermocouples were used in conjunction with thermocouple wells to control the furnace temperature. The control point was adjusted so that the test section would be at the proper temperature. Thus the effect of test environment on thermocouple properties was not a source of error in this procedure.

The type 304 stainless steel creep-test specimens used in these investigations were made from 0.060-in.-thick sheet having the chemical composition indicated in Table 1. All specimens were annealed at 1900°F (1038°C) for 1 hr in hydrogen and prepared from heat M43484 unless otherwise noted.

Table 1. Chemical Composition of Stainless Steel Utilized in CO<sub>2</sub> Compatibility Study

Element	Analyses <sup>a</sup> (wt %)		
	Heat M43484	Heat M33733	Heat C
C	0.067	0.063	0.030
Ni	9.550	9.170	9.530
Cr	18.280	17.640	17.600
Mn	1.180	1.270	1.330
Si	0.540	0.540	0.510
S	0.030 max	0.020 max	0.020 max
P	0.030 max	0.020 max	0.020 max
Mo			0.230
Fe	Balance	Balance	Balance

<sup>a</sup>Vendors' analyses.

## EXPERIMENTAL RESULTS

### Effect of CO<sub>2</sub> on the Creep Properties

The increased time for type 304 stainless steel to rupture at 1500 and 1700°F (815 and 927°C) in flowing CO<sub>2</sub> as compared with argon is shown in Fig. 2. Both wet (dew point, approx 78°F) and dry (dew point, < -30°F) flowing CO<sub>2</sub> environments are represented by a single curve, since no consistent difference in the effect of water vapor on the stress-rupture results could be found for the test time range of 100 to 5000 hr.

A definite decrease in the creep rate at a given stress was observed over a significant stress range for the material tested at 1500°F (815°C) in dry CO<sub>2</sub> as compared with argon. The addition of water vapor to the CO<sub>2</sub> reduced that difference in creep properties at 1500°F (815°C), as shown in Fig. 3, but appeared to have no effect at 1700°F (927°C).

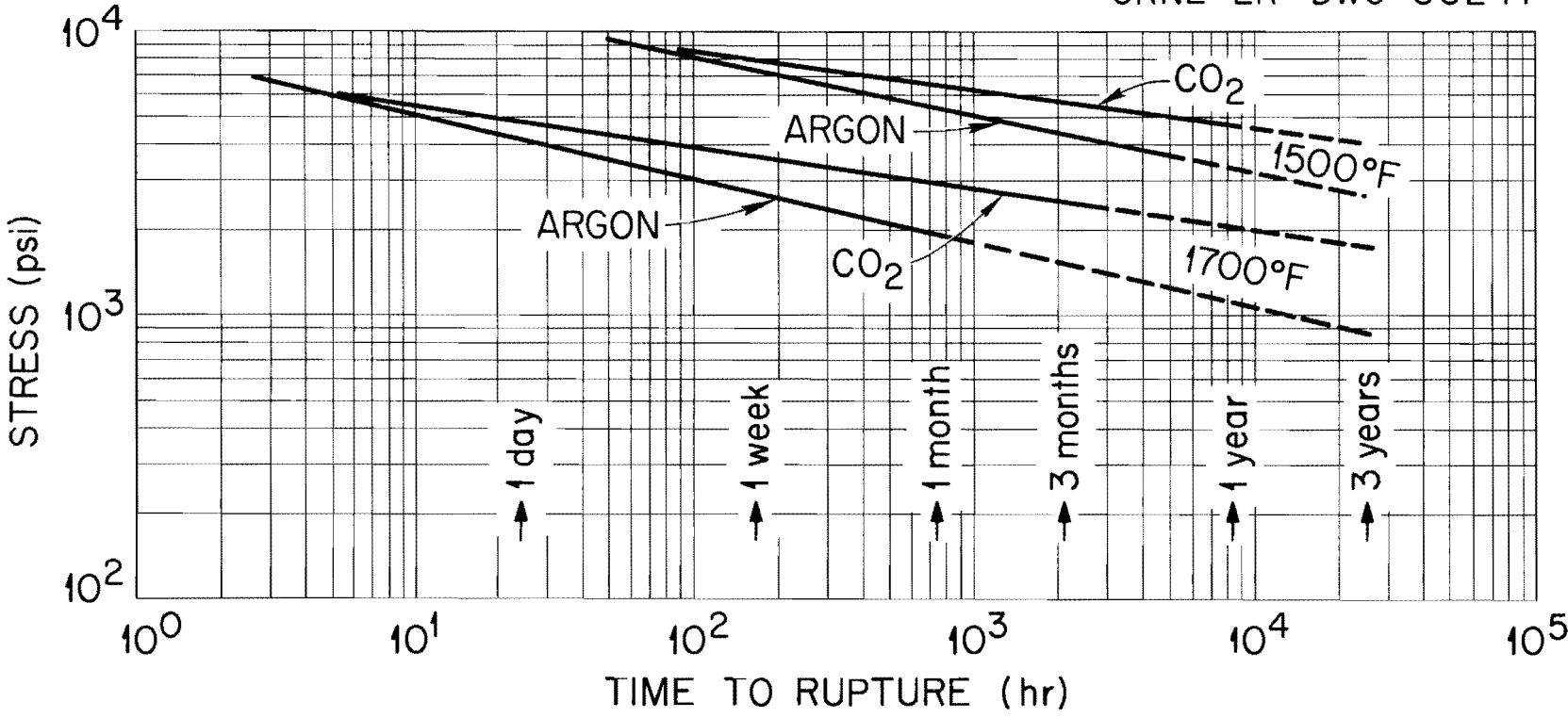


Fig. 2. Environmental Stress Rupture of Type 304 Stainless Steel Tested in Static Argon and Flowing CO<sub>2</sub>.

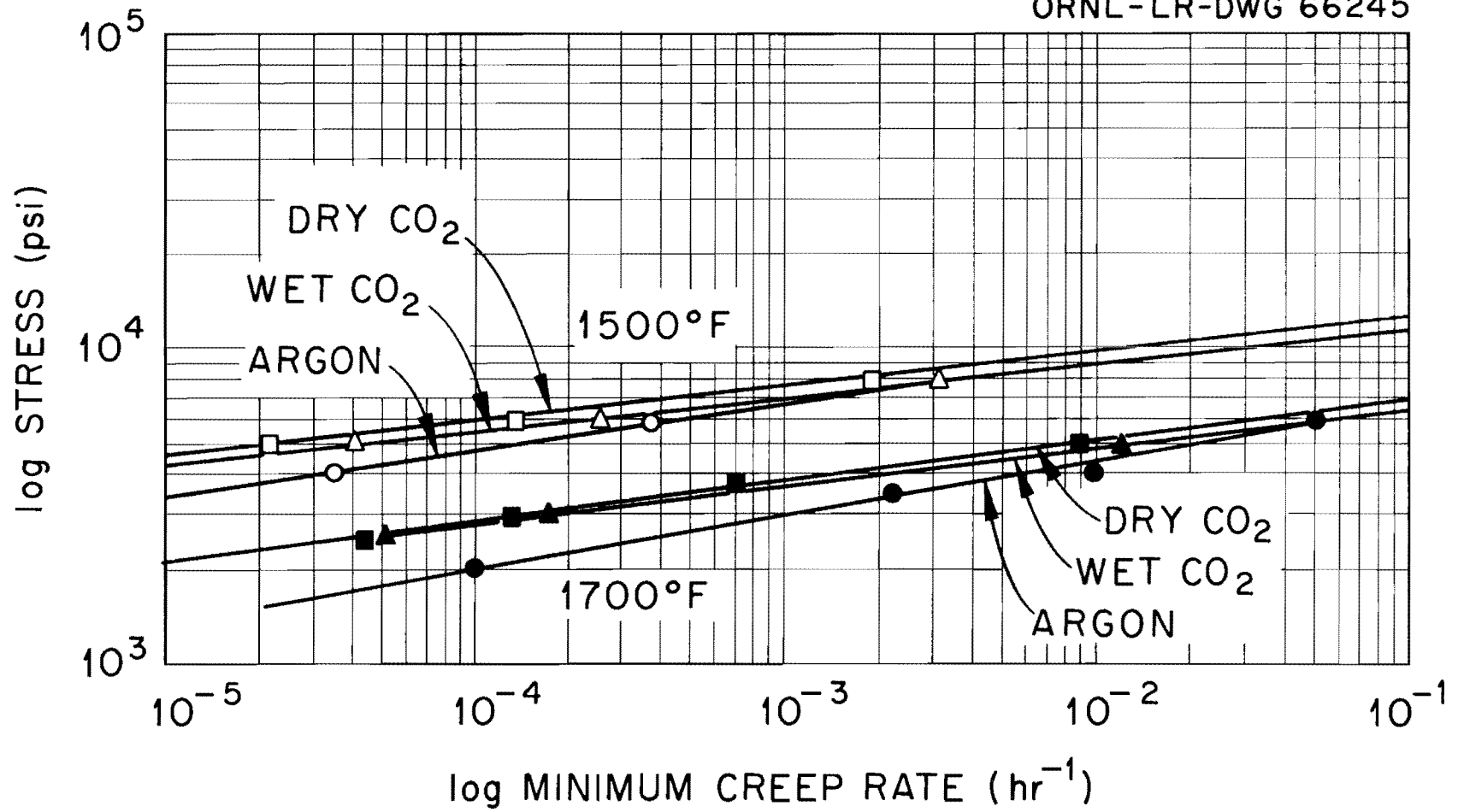


Fig. 3. Stress vs Minimum Creep-Rate Relationship for Type 304 Stainless Steel in Flowing CO<sub>2</sub> Gas and Argon.

The total creep elongation at fracture as a function of time of test is shown in Fig. 4 for argon and dry and wet CO<sub>2</sub> environments at 1500 and 1700°F (815 and 927°C).

#### Effect of Specimen Size on the Stress-Rupture Creep Properties

In the design of components for high-temperature use many sections of material will vary in thickness. Therefore after the creep properties of type 304 stainless steel had been observed to differ significantly when tested in CO<sub>2</sub> and in argon, the effect of specimen size was examined cursorily at 1700°F (927°C). However, as illustrated in Fig. 5, the argon environment is, for all engineering purposes, inert and section size was not a variable when considering the deformation of type 304 stainless steel in that medium. As is also illustrated, such deformation was a function of section thickness when the steel was tested in either dry or wet CO<sub>2</sub> at 1700°F (927°C) under 4000 psi stress. The carbon analyses of these tests in Table 2 indicate increasing carbon content with increasing time at temperature.

Table 2. Carbon Analyses of Type 304 Stainless Steel Creep Specimens of Different Thickness Tested at 1700°F (927°C) in CO<sub>2</sub>

Specimen Thickness (in.)	Rupture Time (hr)	Carbon Analyses <sup>a</sup> (wt %)	
		Dry-CO <sub>2</sub> Environment	Wet-CO <sub>2</sub> Environment
0.060	38.3		0.17
0.040	39.2		0.26
0.060	46.0	0.25	
0.040	61.0	0.21	
0.020	138.1		0.31
0.020	155.0	0.37	
0.020	171.0		0.37

<sup>a</sup>Heat M33733; carbon analysis in as-received condition, 0.063 wt %.

UNCLASSIFIED  
ORNL-LR-DWG 66246

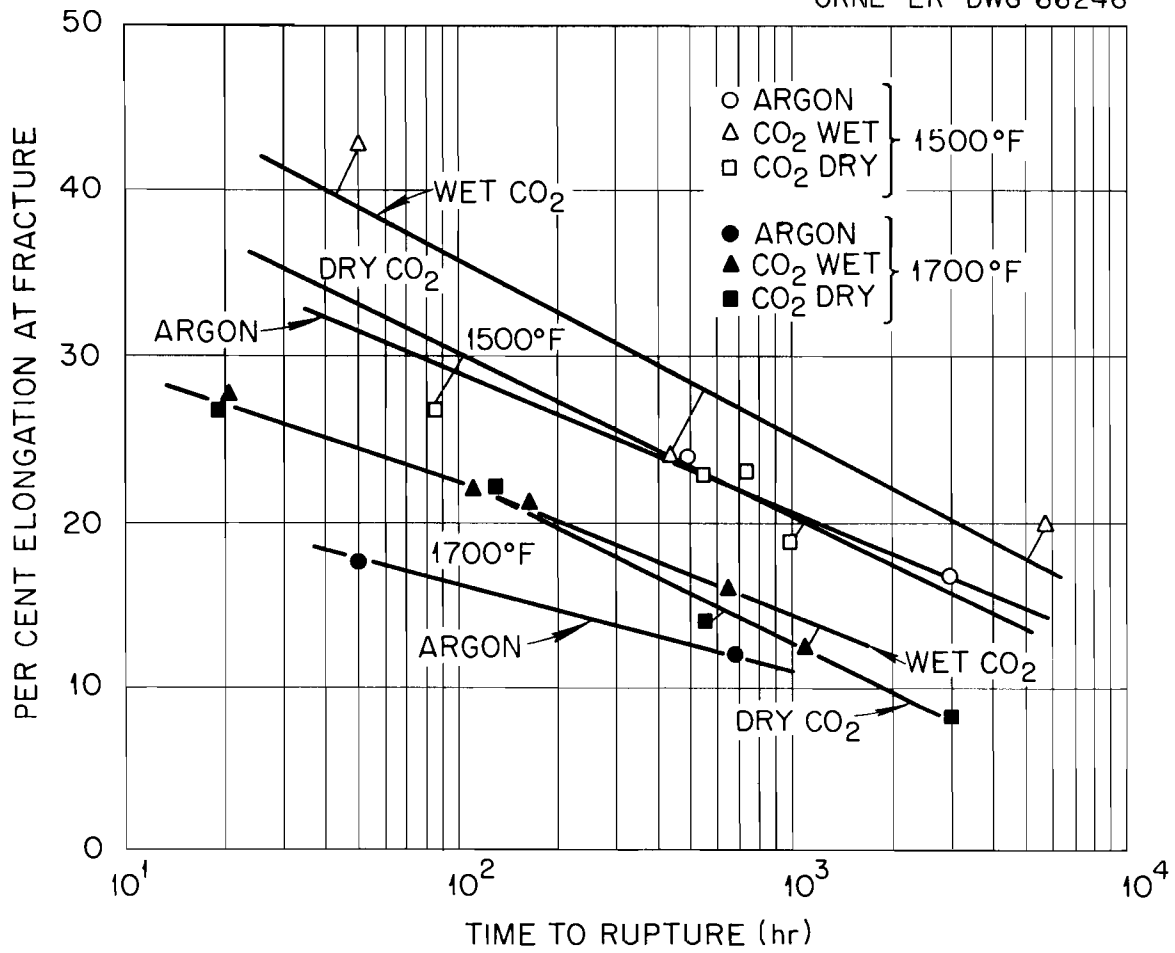


Fig. 4. Elongation at Rupture for Type 304 Stainless Steel at Elevated Temperature.

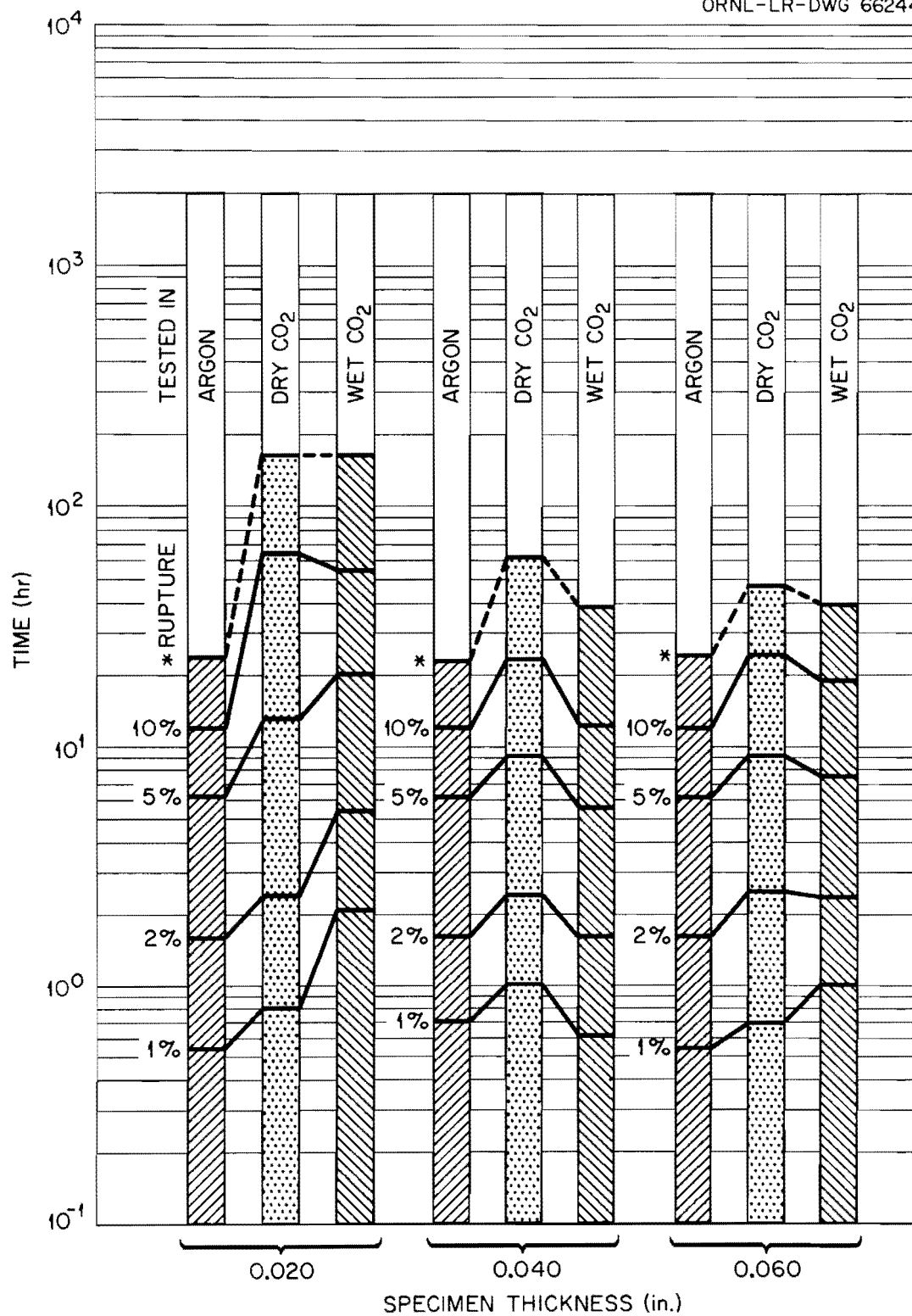


Fig. 5. Effect of Specimen Thickness on the Environmental Creep of Type 304 Stainless Steel at 1700°F (927°C) Under 4000 psi.

Effect of Prestraining on the Creep of Stainless Steel

The effects of CO<sub>2</sub> environment versus those of an inert environment on the creep properties at 1300 and 1500°F (704 and 815°C) of a type 304 stainless steel as a function of prior strain at room temperature are given in Table 3. These data indicate that the creep rate and the fracture strain decreased with increasing prestrain at 1300°F (704°C) and that the time to rupture increased with increasing prestrain.

Table 3. Effect of Environment on the Creep Properties of Prestrained Type 304 Stainless Steel<sup>a</sup> at Elevated Temperature

Environment	Prestrain (%)	Strain at Rupture (%)	Rupture Time (hr)	Creep Rate (hr <sup>-1</sup> )
<u>Tested at 20000 psi at 1300°F (704°C)</u>				
Flowing dry CO <sub>2</sub>	0	18.8	9.8	1.1 × 10 <sup>-2</sup>
	5	13.5	19.6	3.85 × 10 <sup>-3</sup>
	10	11.7	27.9	2.00 × 10 <sup>-3</sup>
	20	5.1	36.8	1.10 × 10 <sup>-3</sup>
Static argon	0	18.8	15.8	1.10 × 10 <sup>-2</sup>
	5	31.3	18.1	1.10 × 10 <sup>-2</sup>
	10	17.4	21.5	1.15 × 10 <sup>-2</sup>
	20	12.1	23.9	2.00 × 10 <sup>-3</sup>
<u>Tested at 7000 psi at 1500°F (815°C)</u>				
Flowing dry CO <sub>2</sub>	0	20.3	148.0	1.00 × 10 <sup>-3</sup>
	5		378.0+	8.20 × 10 <sup>-5</sup>
	10	4.7	432.3	5.70 × 10 <sup>-5</sup>
	20	1.2	162.0	6.00 × 10 <sup>-5</sup>
Static argon	0	20.3	98.2	1.64 × 10 <sup>-3</sup>
	5	12.1	134.4	6.10 × 10 <sup>-4</sup>
	10	4.7	220.9	1.00 × 10 <sup>-4</sup>
	20	1.6	160.7	4.80 × 10 <sup>-5</sup>

<sup>a</sup>Heat M33733.

Similar behavior was observed at 1500°F (815°C) except for a maximum rupture-time value at intermediate values of prestrain. The strain-time curves shown in Fig. 6 illustrate that the primary creep at 1500°F (815°C) was reduced by prestraining but was not significantly different for a given prestrain as a function of environment.

#### Microstructural Changes Associated with Environmental Creep Testing in CO<sub>2</sub>

Photomicrographs of the interior and surface of type 304 stainless steel creep-tested in argon for long periods at either 1500 or 1700°F (815 or 927°C) are shown in Figs. 7 and 8. Typical microstructures of specimens tested in dry or wet CO<sub>2</sub> are shown in Figs. 9 and 10 for 1500°F (815°C) and in Figs. 11 and 12 for 1700°F (927°C). The feather-like structure at the oxide-metal interface revealed in Figs. 11 and 12 reacted to chemical-etching techniques much as ferrite does but has not been positively identified as such. Changes in microstructure in the interior of the creep specimen as a function of time in CO<sub>2</sub> at 1700°F (927°C) are shown in Figs. 13, 14, and 15.

Figure 16 shows an oxide formation that was typical at 1500 or 1700°F (815 or 927°C). An x-ray powder pattern of the extracted oxide showed the presence of alpha-Fe<sub>2</sub>O<sub>3</sub>, Cr<sub>2</sub>O<sub>3</sub>, and Fe<sub>3</sub>O<sub>4</sub>. A glancing-angle x-ray beam on the outer surface of a chipped section of the oxide indicated Fe<sub>3</sub>O<sub>4</sub> only.

#### Influence of CO<sub>2</sub> on the Tensile Properties of Type 304 Stainless Steel

In order to evaluate the influence of CO<sub>2</sub> on the mechanical properties of type 304 stainless steel, a group of tensile specimens were prepared and exposed to flowing CO<sub>2</sub> for times up to 1000 hr and temperatures ranging from 1100 to 1700°F (593 to 927°C). Control specimens were run in argon to separate the influences of thermal treatment and exposure to CO<sub>2</sub>. Pairs of specimens annealed under duplicate conditions were tested in tension at 75 and 1250°F

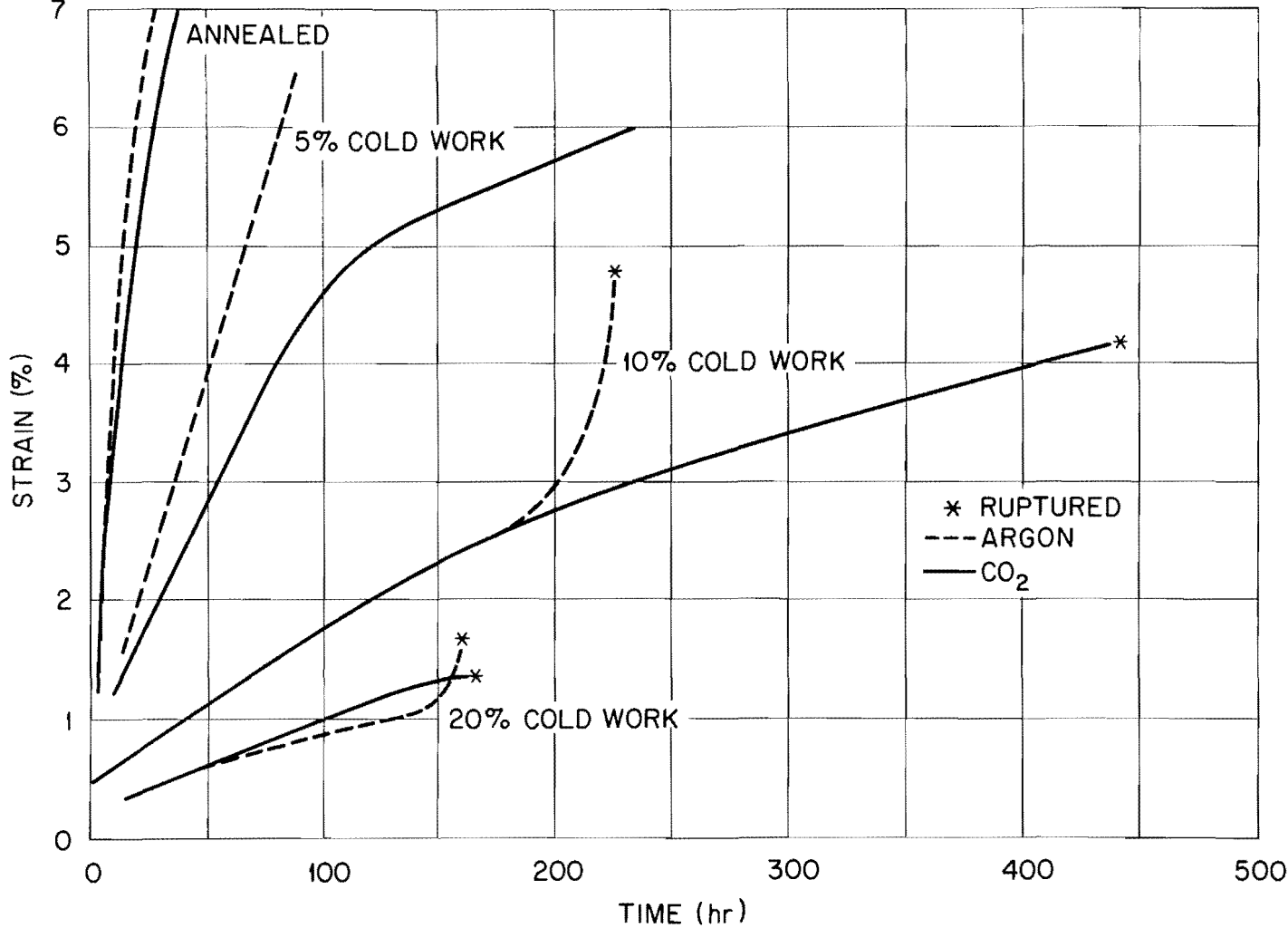


Fig. 6. Effect of CO<sub>2</sub> Environment at 1500°F (815°C) on Creep of Cold-Worked Type 304 Stainless Steel.



Fig. 7. Structure of Type 304 Stainless Steel Creep-Tested for 2869.7 hr at 1500°F (815°C), 4000 psi Stress, in Static Argon. Specimen ruptured at 15.62% strain. Etchant: aqua regia. 100X.

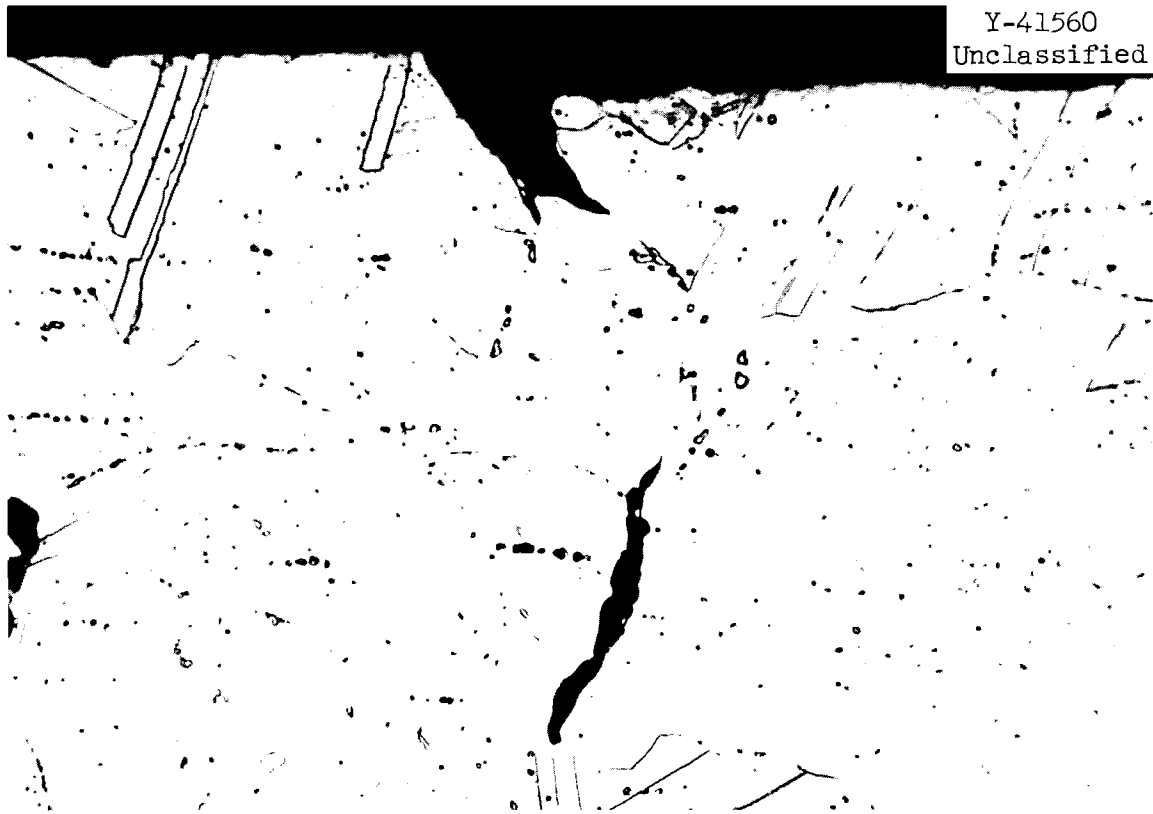


Fig. 8. Surface of Type 304 Stainless Steel as Removed from Creep Testing Apparatus After Extended Service at 1700°F (927°C). An oxide-free surface and intergranular crack formation can be noted. Etchant: aqua regia. 500X.

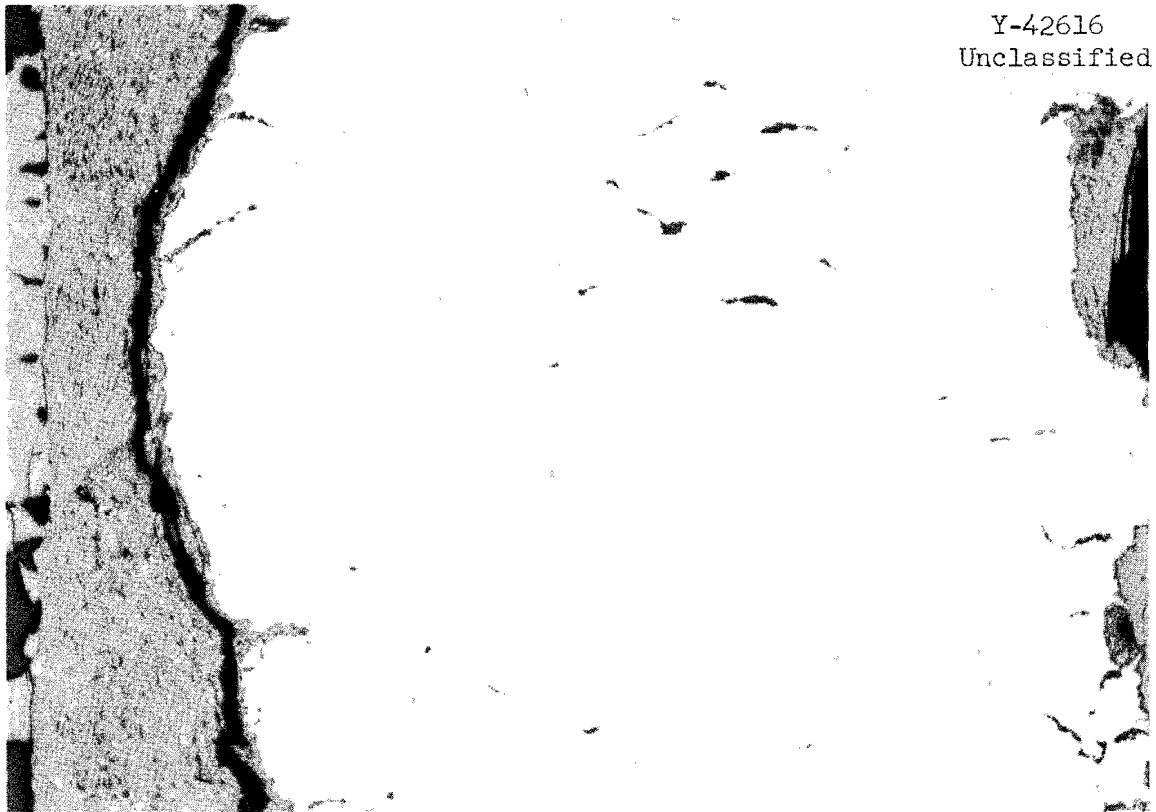


Fig. 9. Microstructure of Type 304 Stainless Steel Creep-Tested for 1200 hr at 1500°F (815°C), 6000 psi Stress in Flowing CO<sub>2</sub>. Photomicrograph typical for material exposed to either wet or dry CO<sub>2</sub> at 1500°F (815°C). Outer oxide spalled off during sample preparation. Etchant: aqua regia. 100X.



Fig. 10. Typical Microstructure of Type 304 Stainless Steel Tested for 1200 hr at 1500°F (815°C) in Flowing Dry CO<sub>2</sub>. Carbon content, 0.29 wt %. Etchant: aqua regia. 500X.

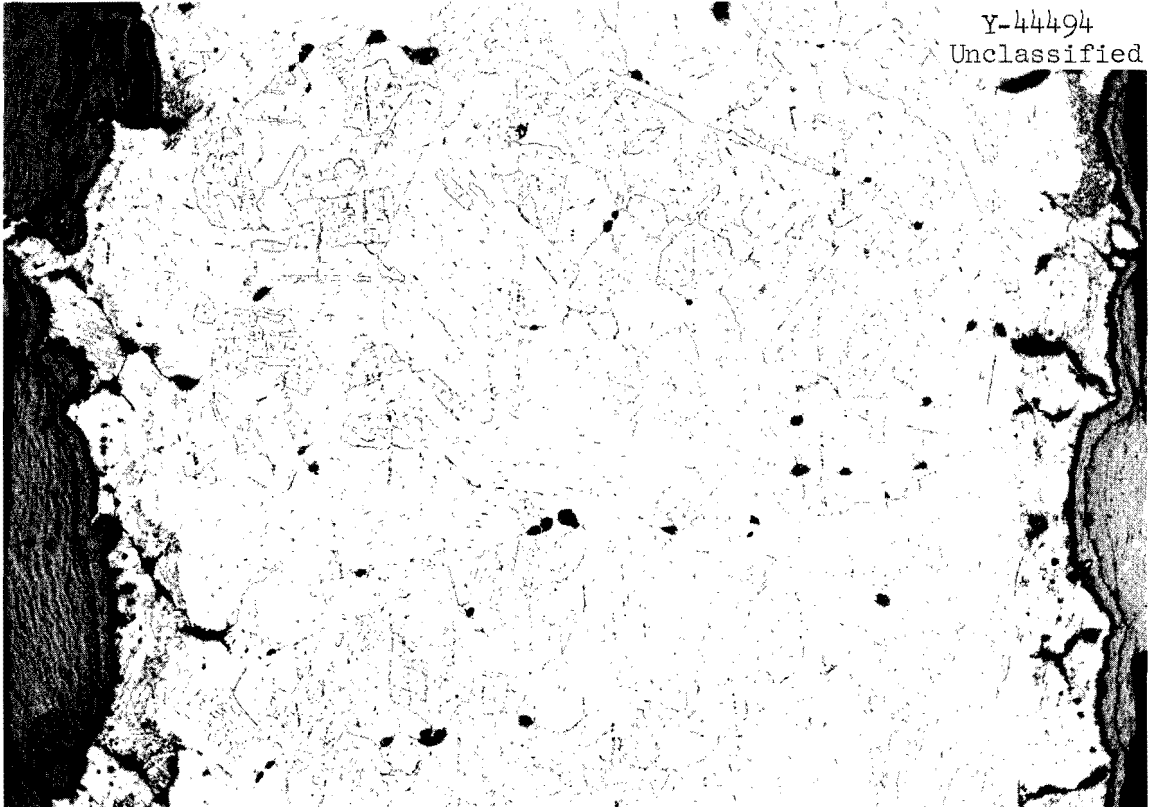


Fig. 11. Typical Microstructure of Type 304 Stainless Steel Tested for 3488.9 hr at 1700°F (927°C), 2500 psi Stress in Flowing Dry CO<sub>2</sub> (Dew Point < -30°F). Specimen ruptured at 6%. Carbon content, 0.4 wt %. Unusual structure at oxide-to-metal interface can be noted. (See Fig. 12) Etchant: aqua regia. 100X.



Fig. 12. High Magnification of Microstructure at Metal-to-Oxide Interface Shown in Fig. 11. The fine precipitate in the grain matrix identified as  $(Cr,Fe)_4C$  and the absence of precipitate in grain-boundary area (0.001 in. wide) near the feather-like structure formed at the oxide-metal interface can be noted. Etchant: aqua regia. 500X.

Y-42272  
Unclassified

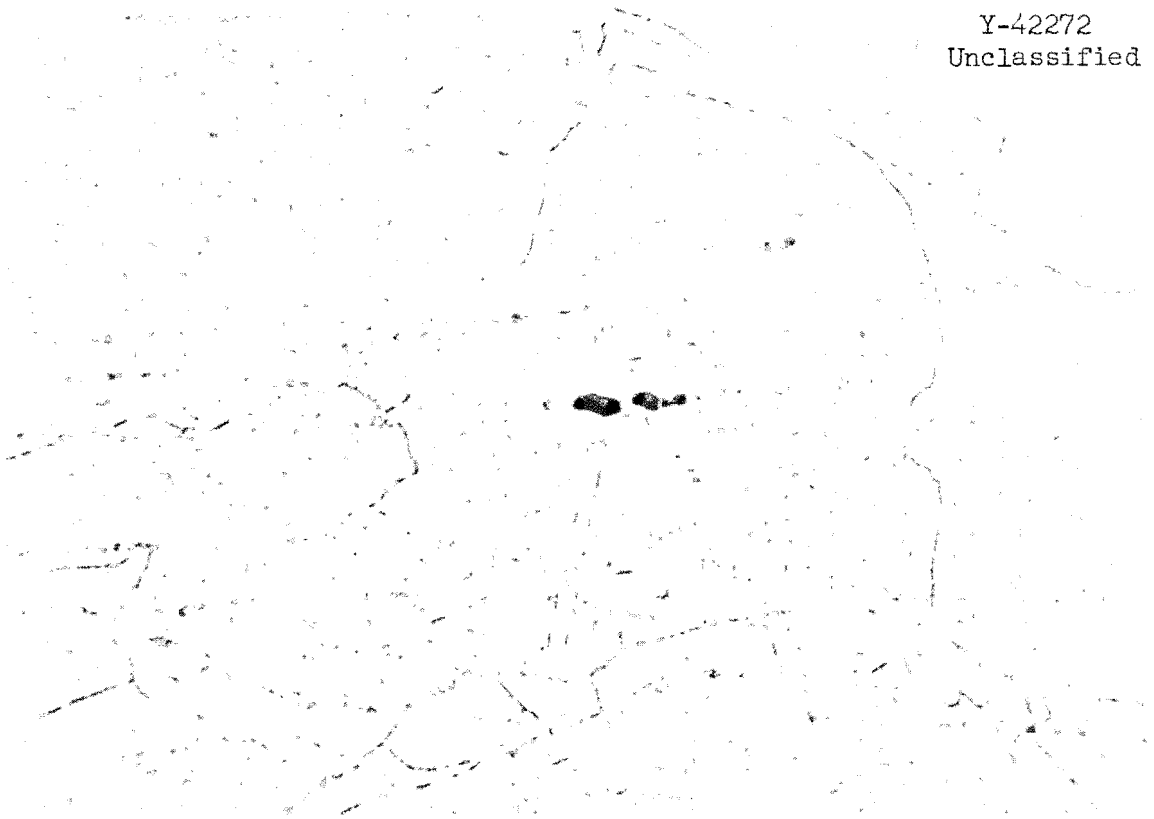


Fig. 13. Typical Microstructure in Interior of Type 304 Stainless Steel Specimen Tested for 18.8 hr at 1700°F (927°C), 5000 psi in Flowing Dry CO<sub>2</sub> (Dew Point < -30°F). Carbon content, 0.30 wt %. Etchant: aqua regia. 500X.

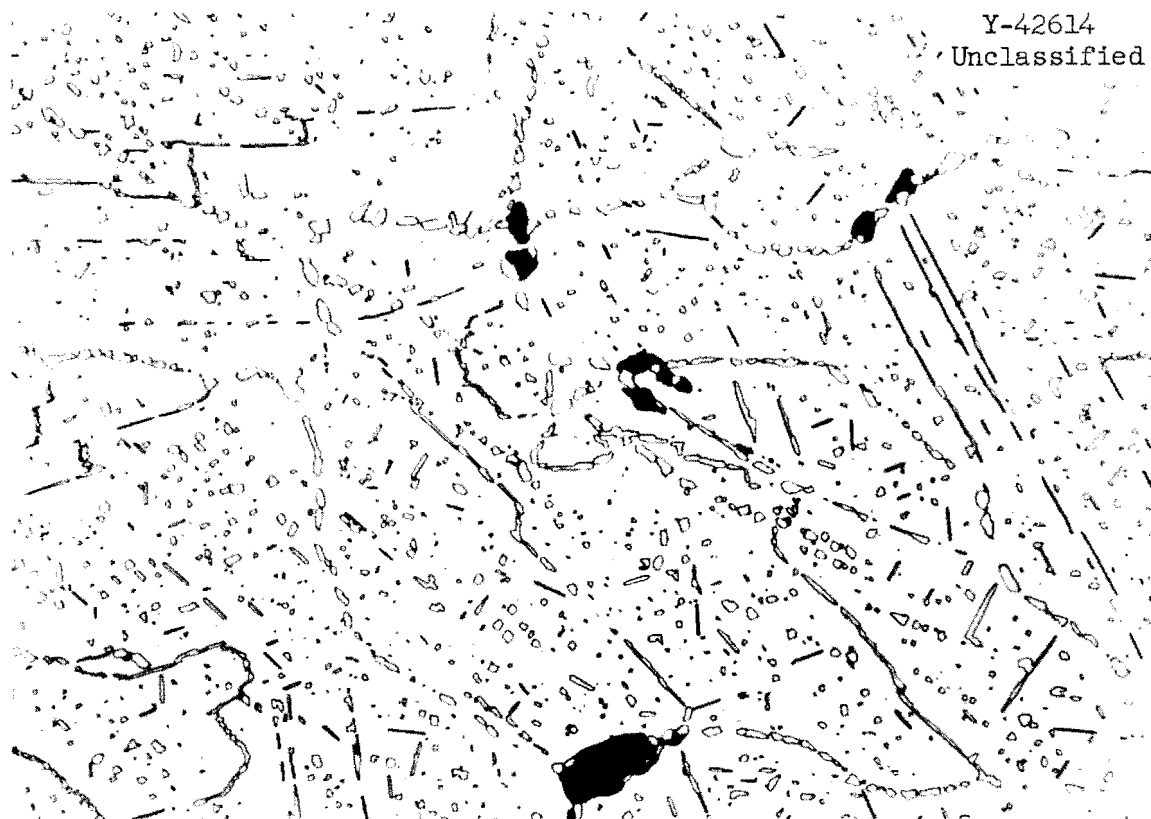


Fig. 14. Typical Microstructure in Interior of Type 304 Stainless Steel Specimens Tested for 528 hr at 1700°F (927°C), 3000 psi Stress in Flowing Dry CO<sub>2</sub> (Dew Point < -30°F). Carbon content, 0.59 wt %. Etchant: aqua regia. 500X.

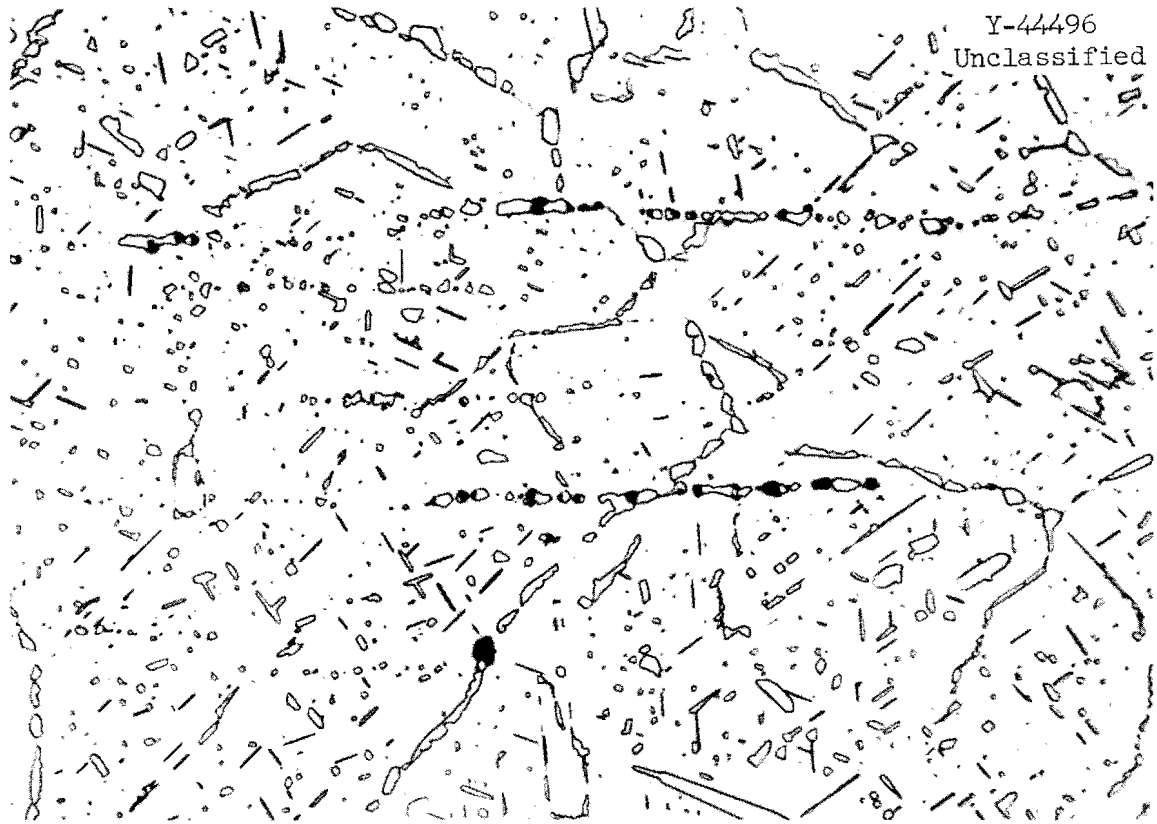


Fig. 15. Typical Microstructure in Interior of Type 304 Stainless Steel Specimen Tested for 3488.9 hr at 1700°F (927°C), 2500 psi Stress in Flowing Dry CO<sub>2</sub> (Dew Point < -30°F). Specimen ruptured at 6%. Carbon content, 0.4%. Large quantities of grain-boundary precipitate and precipitate on particular orientation in the grain interior can be observed. Etchant: aqua regia. 500X.

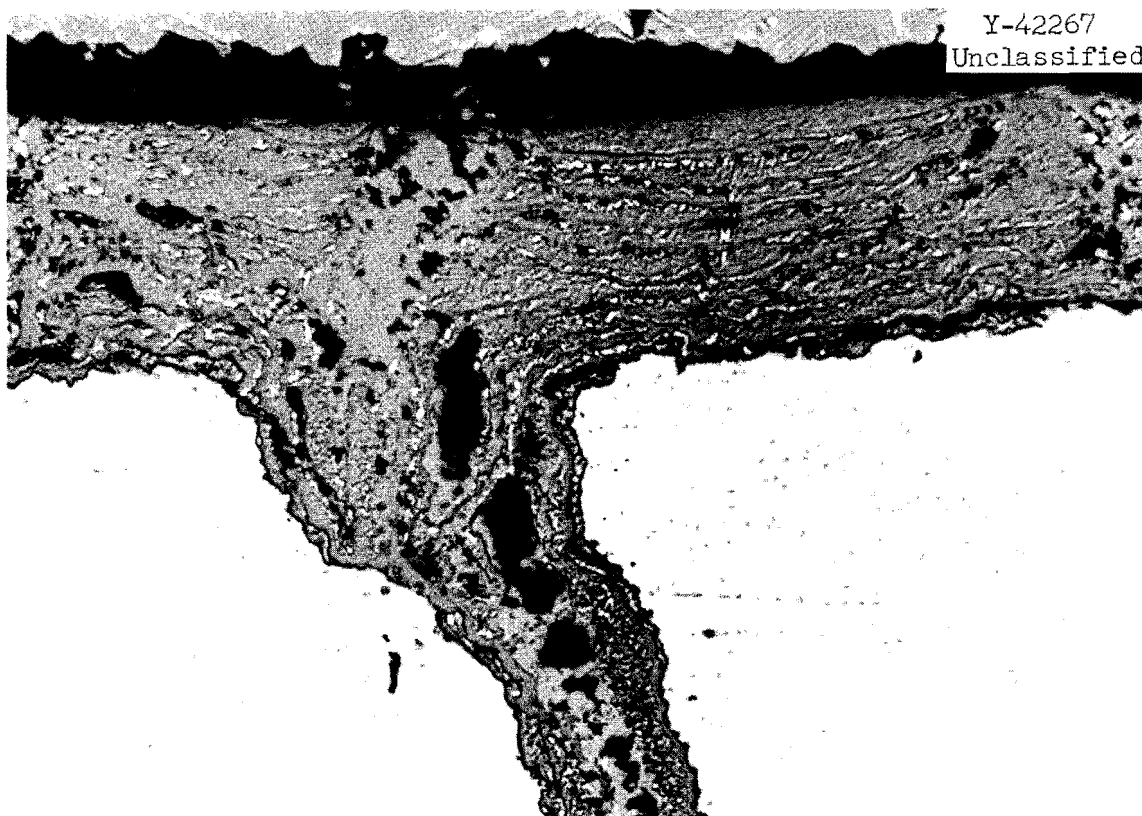


Fig. 16. Typical Type 304 Stainless Steel Surface After Long Exposure to  $\text{CO}_2$  at Elevated Temperatures. Particular specimen exposed 1058 hr at  $1500^\circ\text{F}$  ( $815^\circ\text{C}$ ) in dry  $\text{CO}_2$ . Outer single-phase oxide and interior oxide spinel which contains metallic particles are apparent. As-polished specimen. 500X.

(25 and 677°C); the results are summarized in Table 4. The following observations were made relative to the influence of CO<sub>2</sub> on the tensile ductility:

1. The control specimens showed that subsequent heating in argon at a temperature less than the 1900°F (1038°C) homogenization temperature caused a change in the material characteristics. As a result of this instability, the room-temperature tensile ductility was reduced. The tensile ductility of the controls at 1250°F (677°C) was increased by the thermal treatment, the magnitude of the improvement increasing with increasing annealing temperature.

2. At both 75 and 1250°F (25 and 677°C) the tensile ductility was decreased by exposure to CO<sub>2</sub>. The magnitude of the decrease in ductility seemed, as a result of a given annealing time, to increase with the temperature of annealing.

#### Strengthening Effect

The resistance of type 304 stainless steel to creep deformation was higher in CO<sub>2</sub> than in argon. Material tested in CO<sub>2</sub> showed two definite microstructural changes: increased precipitation and the formation of oxide layers on the metal surface.

Carbon dioxide is strongly oxidizing to type 304 stainless steel at 1500°F (815°C) and above, and the presence of oxygen in solid solution in the austenite, as an oxide coating on the metal surface, or in the metal substrate as metal oxides may constitute a strengthening effect. To investigate this possibility, the effect on the creep properties of the steel of small partial pressures of oxygen in an argon carrier gas was studied. Experiments duplicated with two different heats of the steel produced the same type of results as shown in Figs. 17 and 18. The increased creep strength at small partial pressures of oxygen in argon as compared with either pure argon or pure oxygen was not accompanied by microstructural changes apparent at magnification of 1000 diameters or less. However, electron micrographs at magnifications of 4650 (Figs. 19-22) revealed a higher density of

Table 4. Effects of Exposure to CO<sub>2</sub> on the Tensile Properties of Type 304 Stainless Steel

Specimen Size: 0.020-in.-thick sheet  
Strain Rate: 0.02 in./in.-min

Treatment Prior to Tensile Test <sup>a</sup>			Average Carbon Concentration (wt %)	Tensile Properties at 75°F (25°C)			Tensile Properties at 1250°F (677°C)		
Environment	Temperature	Time (hr)		Elongation (%)	Strength (psi)	Yield Strength (psi)	Elongation (%)	Strength (psi)	Yield Strength (psi)
As annealed			0.02	56.5	80,300	22,300	27.5	34,000	10,100
CO <sub>2</sub>	1100°F (593°C)	100		55.0	86,100	26,300	23.5	34,800	10,000
		300		45.3	83,000	27,200	19.5	34,800	12,800
		1000	0.14	41.6	82,900	28,500	21.5	36,600	12,200
Ar	1100°F (593°C)	1003	0.02	55.0	84,800	25,800	29.5	37,700	14,200
CO <sub>2</sub>	1200°F (649°C)	97.6		53.8	85,100	23,500	27.5	37,200	12,700
		329		56.3	87,800	26,700	26.0	39,200	13,800
		1002	0.15	45.3	88,400	28,000	17.0	42,100	15,700
CO <sub>2</sub>	1300°F (704°C)	500	0.21	25.7	81,600	25,600	17.0	40,100	19,400
		785		25.7	82,700	27,200	17.0	37,900	18,200
		1000	0.27	24.5	83,700	28,200	14.5	39,300	19,300
Ar	1300°F (704°C)	1006	0.02	49.0	83,800	24,300	29.0	37,500	12,000
CO <sub>2</sub>	1400°F (760°C)	303		20.9	70,100	26,900	15.0	35,300	18,000
		500		14.8	70,500	29,100	14.0	31,500	15,300
		1000	0.25	20.9	77,200	29,000			20,300
CO <sub>2</sub>	1500°F (815°C)	25	0.21	38.0	79,400	23,100	18.5	35,800	13,000
		115		27.5	77,900	23,100	19.0	36,400	17,200
		500	0.25	19.5	80,600	25,900	16.5	37,700	19,100
Ar	1500°F (815°C)	500	0.02	53.0	84,500	25,100	34.0	38,700	11,300
CO <sub>2</sub>	1700°F (927°C)	16.7	0.12	41.6	64,400	21,400	21.0	36,900	15,100
		49.2		22.1	60,100	21,800	17.0	33,000	15,100
		200	0.22	11.1	45,000	18,400	12.0	28,000	9,900
Ar	1700°F (927°C)	200	0.02	54.5	83,700	24,400	36.0	35,800	11,100

<sup>a</sup>All specimens annealed for 1 hr at 1900°F (1038°C) in hydrogen prior to receiving indicated treatment.

UNCLASSIFIED  
ORNL-LR-DWG 51625

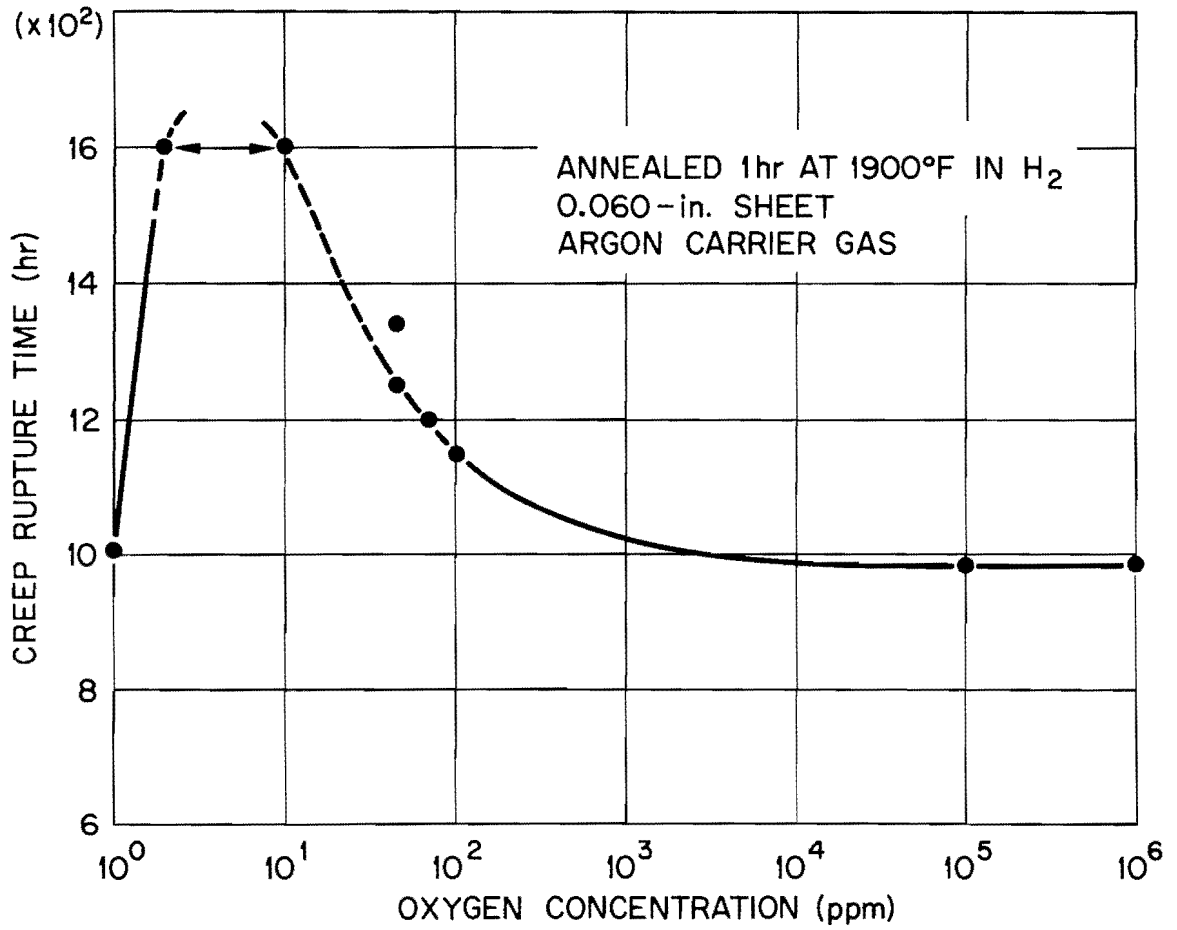


Fig. 17. Effect of O<sub>2</sub> Concentration on the Rupture Life of Type 304 Stainless Steel at 1500°F (815°C) and 3400 psi.

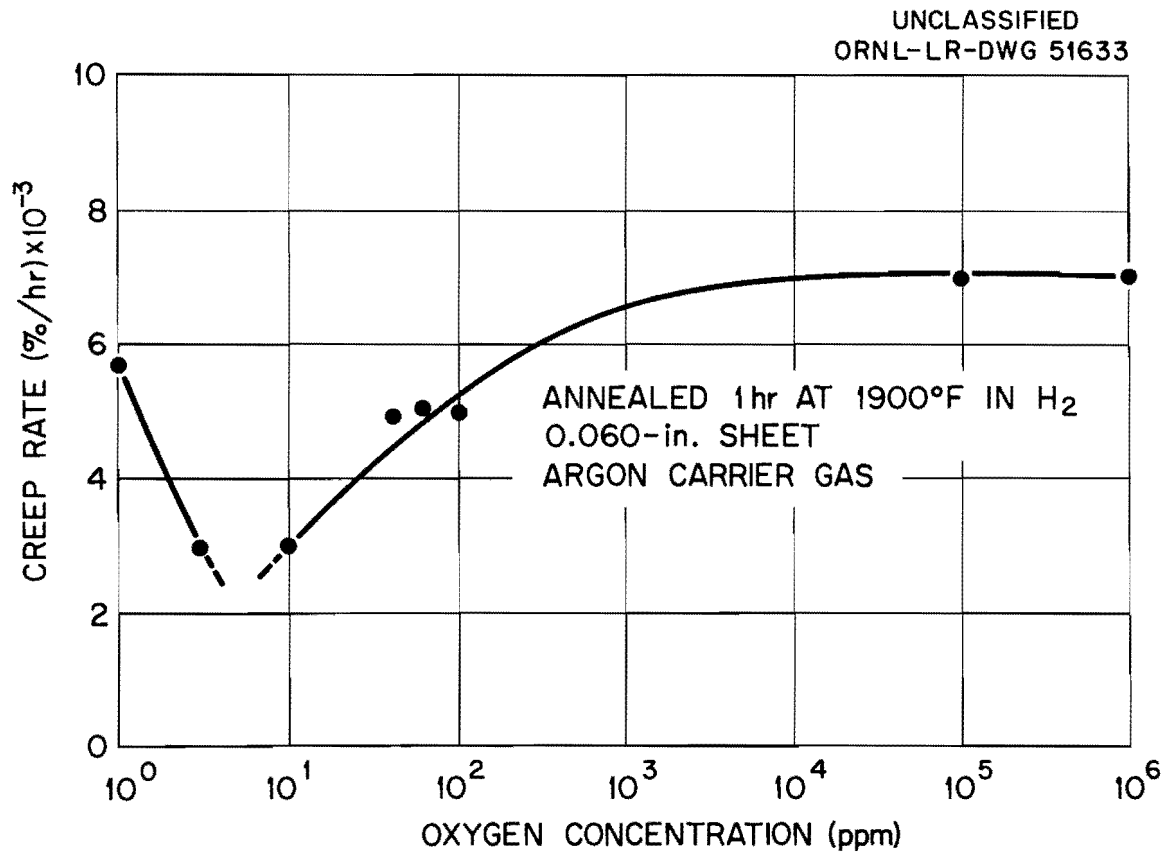


Fig. 18. Effect of O<sub>2</sub> Concentration on the Creep Rate of Type 304 Stainless Steel at 1500°F (815°C) and 3400 psi.

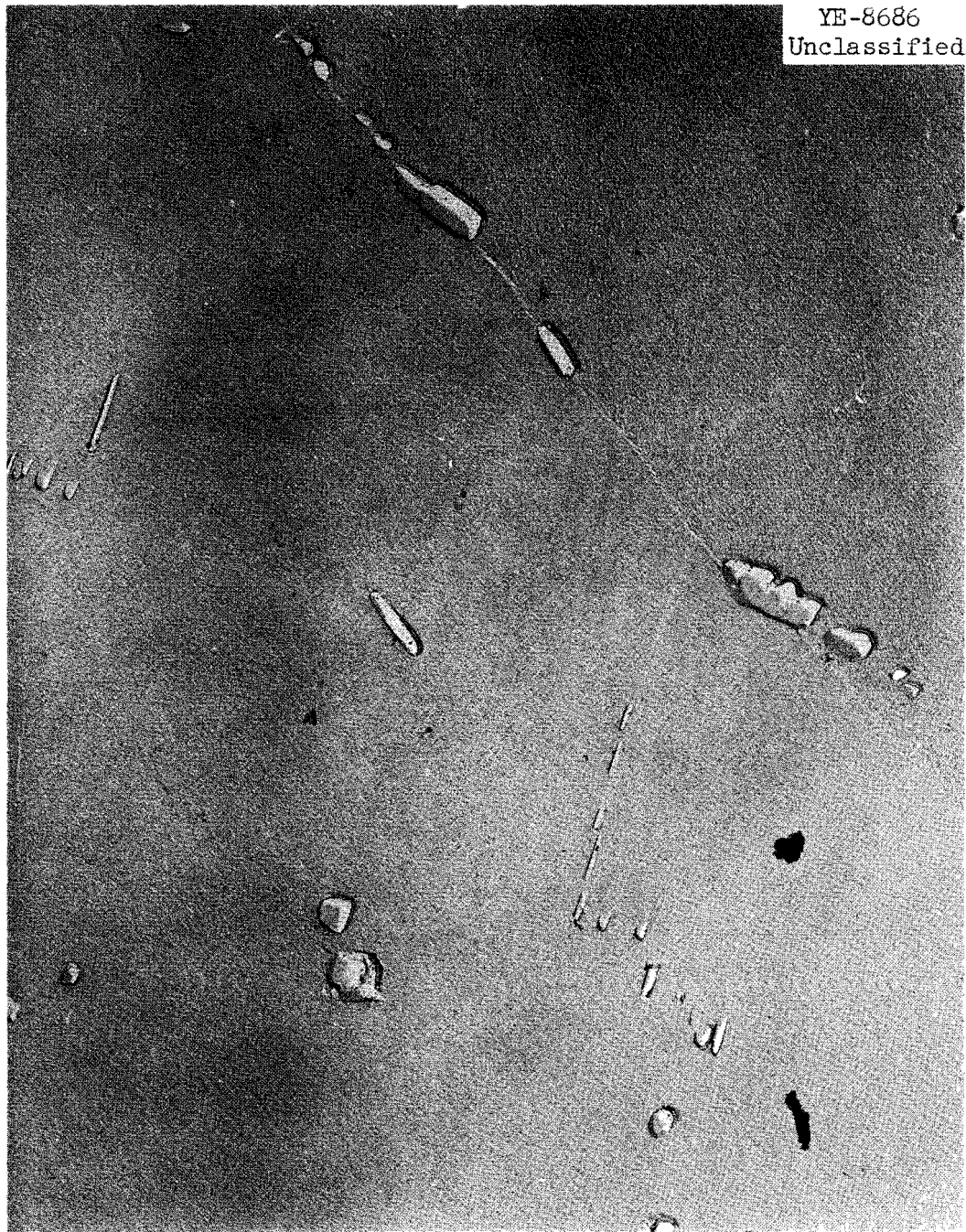


Fig. 19. Microstructure of Type 304 Stainless Steel (Heat C) Stressed at 3500 psi, 1500°F (815°C) for 1000 hr in Static Argon. Electron photomicrograph. 4650X.

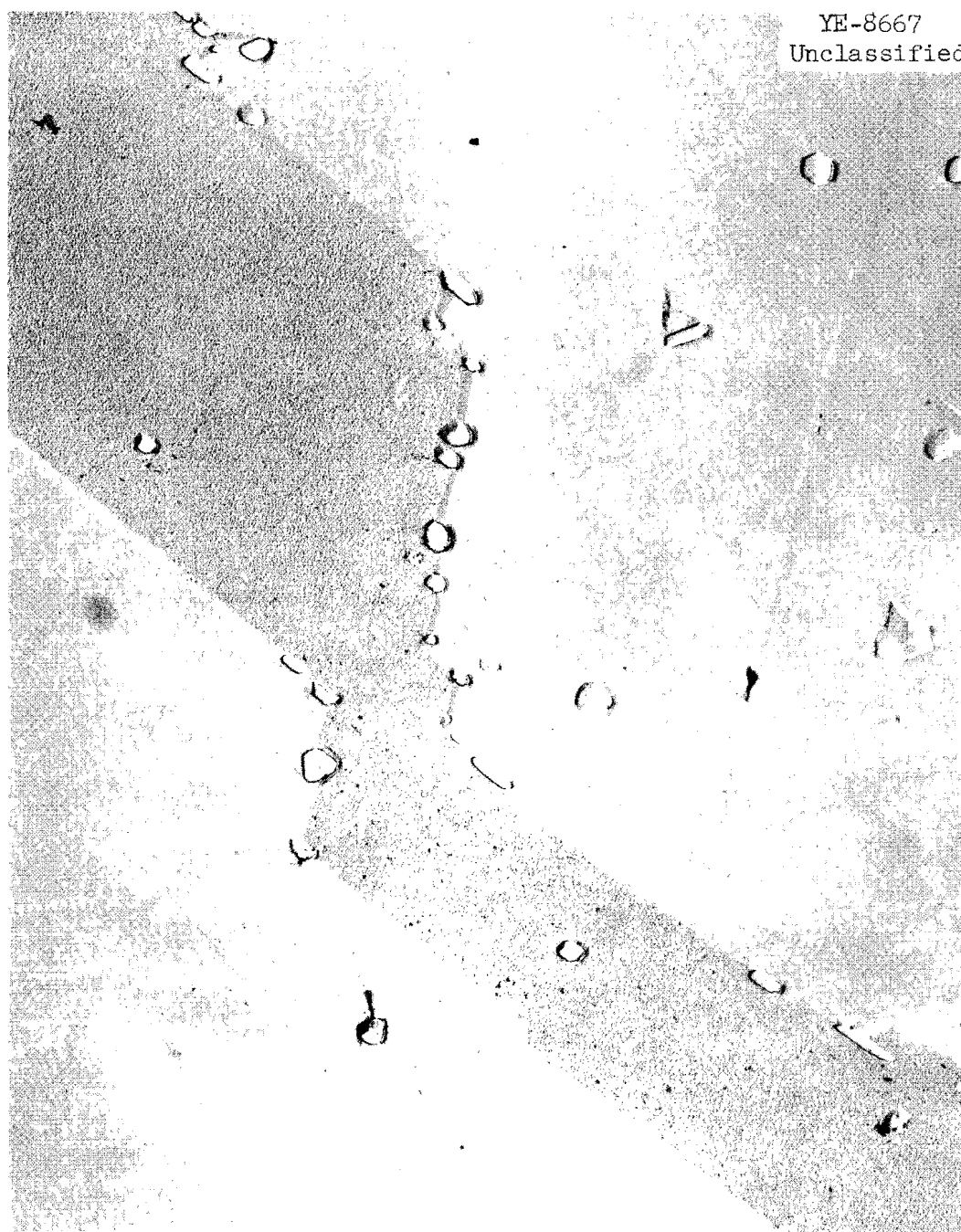


Fig. 20. Typical Microstructure of Type 304 Stainless Steel (Heat C) Stressed at 3500 psi, 1500°F (815°C) for 1600 hr in Flowing Argon-Oxygen Gas Mixture. Oxygen concentration in environment varied from 0.0002 to 0.001 vol %. Electron photomicrograph. 4650X.

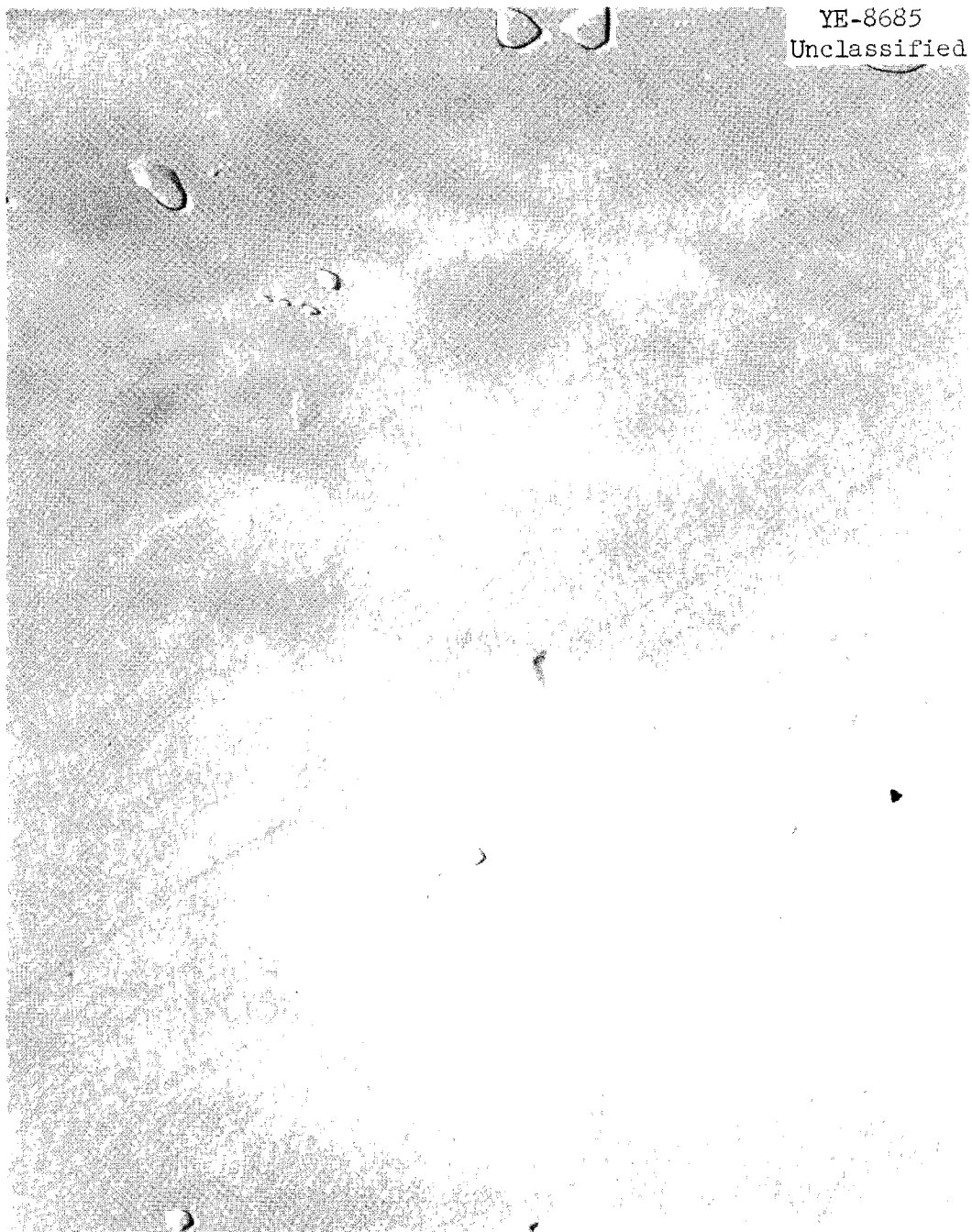


Fig. 21. Microstructure of Type 304 Stainless Steel (Heat C) Stressed at 3500 psi, 1500°F (815°C) for 980 hr in Flowing Argon-Oxygen Gas Mixture. Oxygen concentration in environment was 12 vol %. Electron photomicrograph. 4650X.



Fig. 22. Microstructure of Type 304 Stainless Steel (Heat C) Stressed at 3500 psi, 1500°F (815°C) for 979 hr in Flowing Oxygen. Electron photomicrograph. 4650X.

precipitate at the lower concentrations of oxygen when compared with 12% O<sub>2</sub> in argon or with the 100% O<sub>2</sub> atmosphere. A closer examination of a number of the tests revealed that the maximum effect on strength was achieved with a concentration of approximately 10 ppm O<sub>2</sub> in argon. The increase in oxygen concentration in the metal substrate after an exposure of 1600 hr in this optimum Ar-O<sub>2</sub> environment at 1500°F (815°C) was insignificant.

It was evident from the surface oxides that the oxidizing potential of the CO<sub>2</sub> at 1500 and 1700°F (815 and 927°C) was greater than the oxidizing potential of the Ar-O<sub>2</sub> mixture causing the maximum creep properties. Therefore it must be concluded that oxygen may contribute to the strengthening mechanism but cannot be primarily responsible for the effect noted for stainless steel tested in CO<sub>2</sub>.

The increased precipitate in material tested in CO<sub>2</sub> led to the suspicion that carburization of the metal matrix had occurred. Chemical analyses indicated that the change in carbon content followed a general trend of increasing with increasing time and temperature. To further study this carburization phenomenon, stainless steel tabs were annealed in flowing CO<sub>2</sub> in a nonmetallic loop where all metallic materials except the specimen were removed. The CO<sub>2</sub>, produced by decomposition of BaCO<sub>3</sub>, contained C<sup>14</sup> as a tracer. Autoradiographs of the stainless steel tabs after exposure to the CO<sub>2</sub> at 1300, 1500, and 1700°F (704, 815, and 927°C) are shown in Figs. 23, 24, and 25, respectively. Figure 26 shows the distribution of carbon at the oxide-metal interface. Beta-counting techniques also indicated that the maximum carbon content was at the oxide-metal interface, with a small concentration present in the inner oxide and no C<sup>14</sup> in the outer oxide. The carburization of the material in pure flowing CO<sub>2</sub> was clearly demonstrated by this technique.

Additional evidence of carburization was obtained by exposure of thin tabs of metal to nonisotopic flowing CO<sub>2</sub>. Typical carbon analyses are shown in Table 5.



Fig. 23. Autoradiograph of Type 304 Stainless Steel Heat Treated for 40 hr in Flowing  $C^{14}O_2$  Environment at 1300°F (704°C). Carbon content, 0.041 wt %. Specimen as polished, NTB stripping radiographic film exposed for 168 hr. 200X.

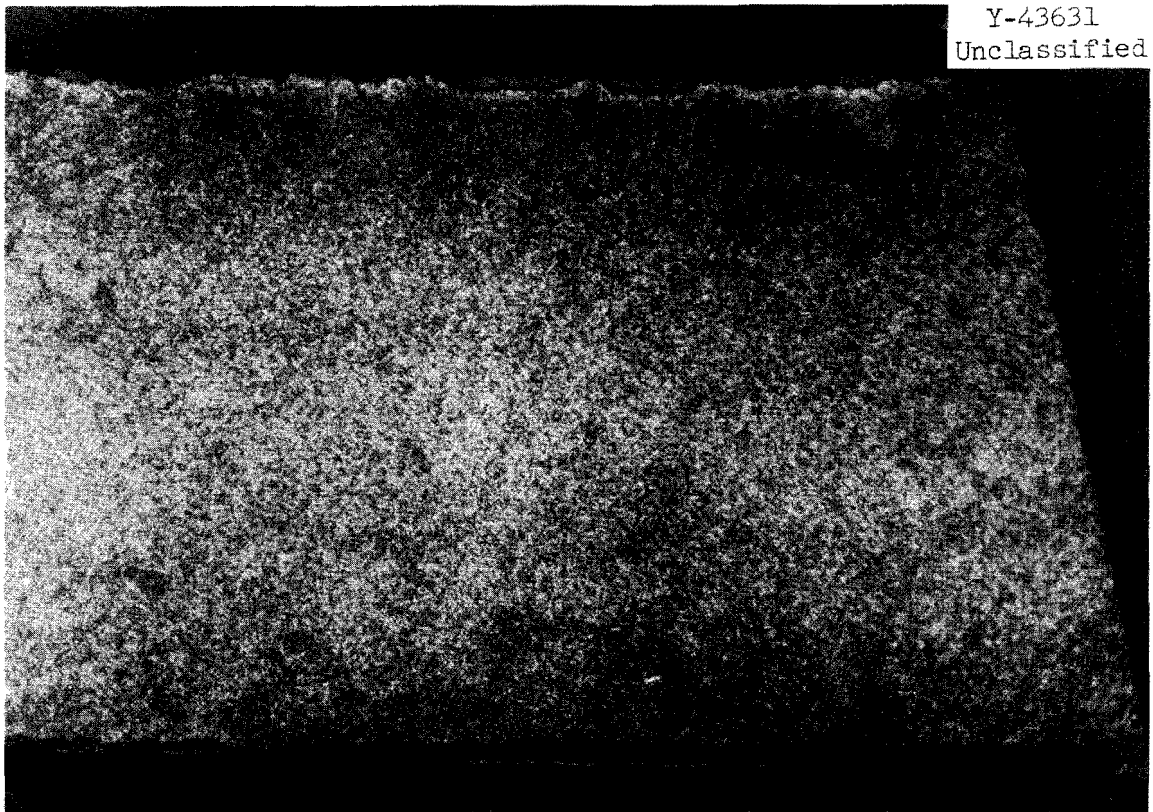


Fig. 24. Autoradiograph of Type 304 Stainless Steel Heat Treated for 40 hr in Flowing  $C^{14}O_2$  Environment at 1500°F (815°C). Carbon content, 0.062 wt %. Specimen as polished, NTB stripping radiographic film exposed for 168 hr. 200X.

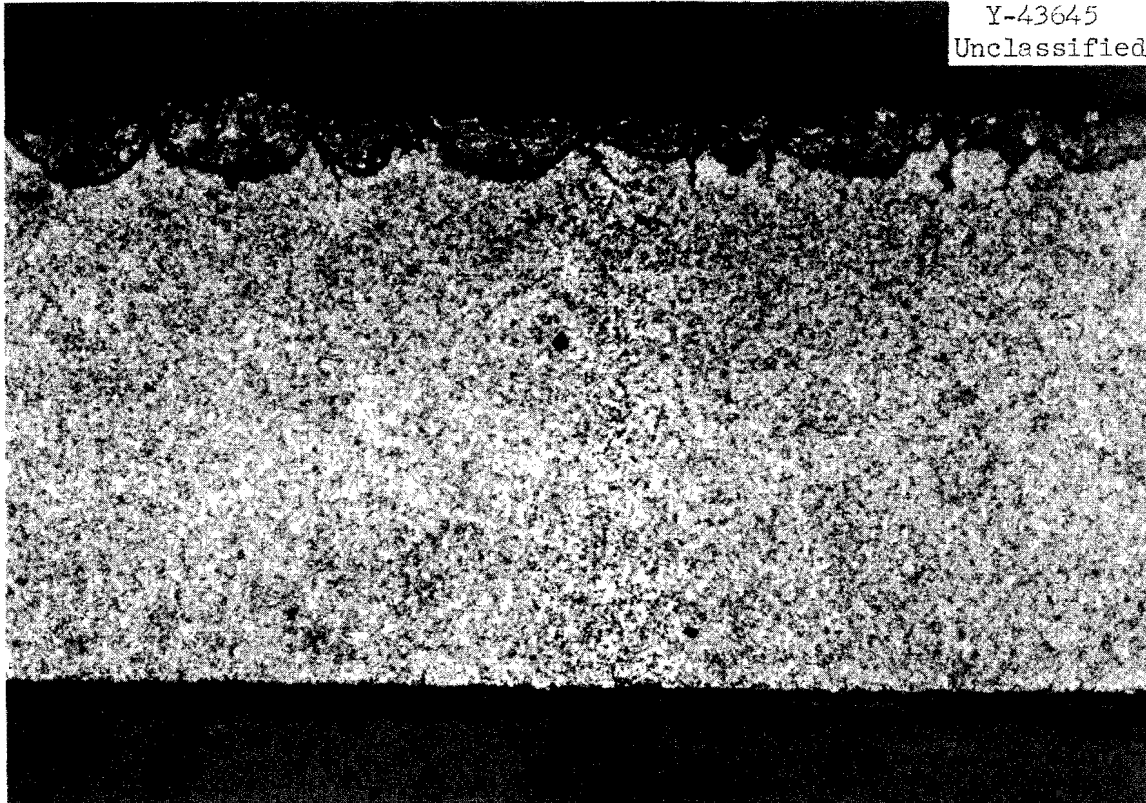
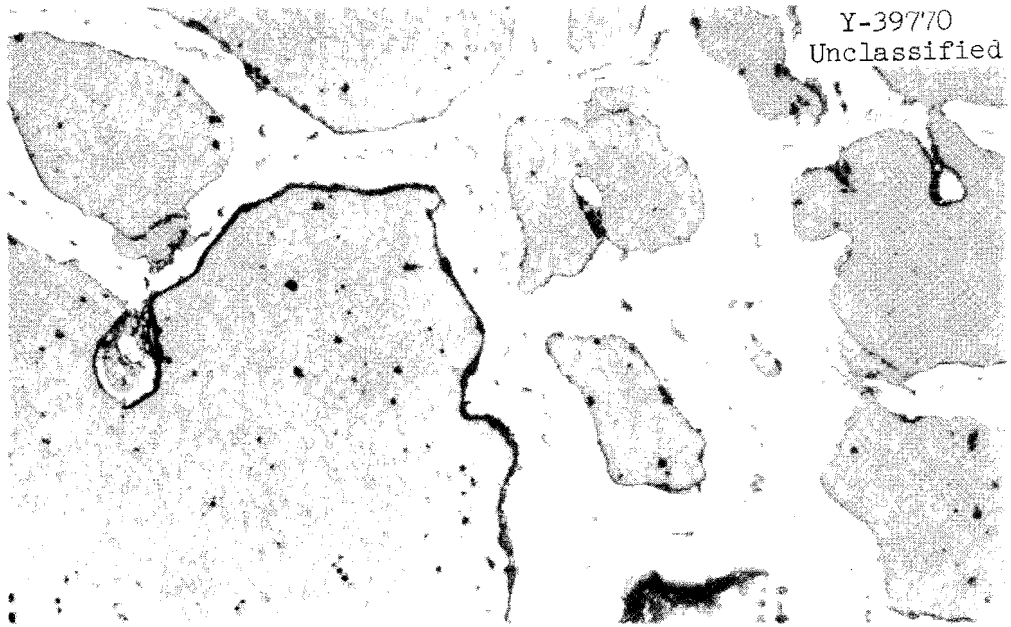
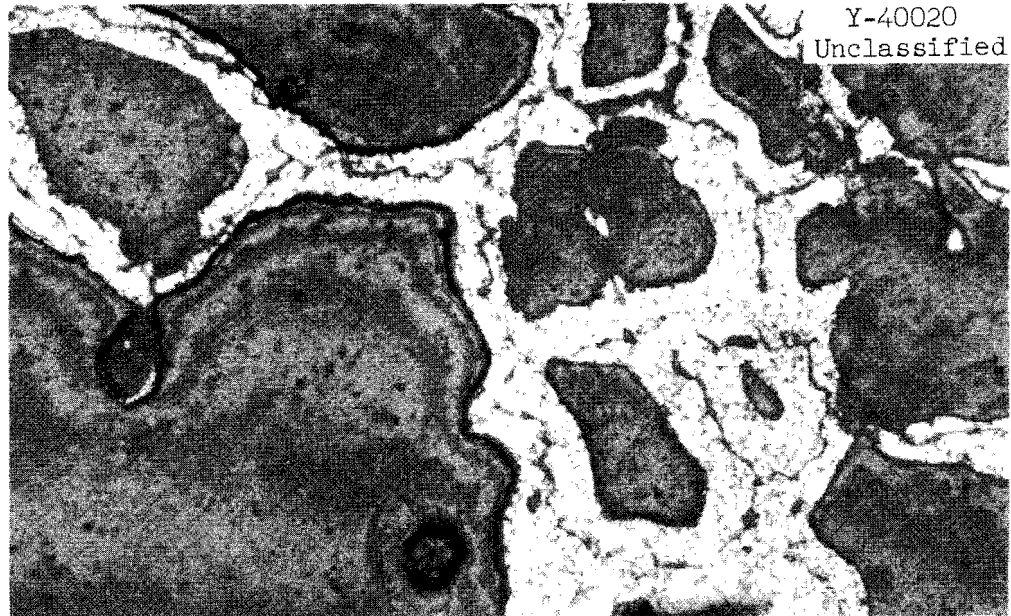


Fig. 25. Autoradiograph of Type 304 Stainless Steel Heat Treated for 40 hr in Flowing  $C^{14}O_2$  Environment at 1700°F (927°C). Gas content, 0.073 wt %. Specimen as polished, NTB stripping radiographic film exposed for 168 hr. 200X.



As-Polished Specimen, 500X



Autoradiograph, 500X

Fig. 26. Representative Structure 0.001 in. from Metal Surface of Type 304 Stainless Steel Specimen ( $0.020 \times 1/2 \times 1$  in.) Exposed 37.8 hr at  $1500^{\circ}\text{F}$  ( $815^{\circ}\text{C}$ ) in Flowing  $\text{C}^{14}\text{O}_2$  Environment. Total surface beta count of specimen 6226 cpm.

Table 5. Carburization of Type 304 Stainless Steel  
in Flowing CO<sub>2</sub> at 1 atm Pressure

Temperature [°F (°C)]	Time (hr)	Carbon Content (wt %)
1200 (649)	50.2	0.07
	94.1	0.12
1300 (704)	138.7	0.30
1400 (760)	49.5	0.24
1500 (815)	46.0	0.30
1600 (871)	50.0	0.37
1700 (927)	69.4	0.44
1800 (982)	48.9	0.21

#### DISCUSSION OF RESULTS

The evidence obtained in the tests supported the suspicion that the strengthening observed in CO<sub>2</sub> was due to carburization rather than oxidation. The strengthening mechanism of carbon was due to solid-solution alloying and/or a dispersed second phase. An explanation of both mechanisms can be found elsewhere.<sup>1,2</sup>

The effect of prestraining at room temperature on the creep properties of an austenitic stainless steel tested in the sensitizing temperature range in an air environment was investigated by Garofalo *et al.*<sup>3</sup> These investigators, whose experimental results showed the same general trends as the data reported in Table 3, concluded that

---

<sup>1</sup>E. R. Parker and T. H. Hazlett, "Principles of Solution Hardening," pp 30-70 in Relation of Properties to Microstructure, American Society for Metals, Cleveland, 1954.

<sup>2</sup>J. Wertman, Theory of Creep of Dispersion-Hardened Alloys, Naval Research Laboratory, NRL-5123 (Apr. 15, 1958).

<sup>3</sup>F. Garofalo, F. von Gemmingen, and W. F. Domis, "The Creep Behavior of an Austenitic Stainless Steel as Affected by Carbides Precipitated on Dislocations," Trans. Am. Soc. Metals 54, 430 (1961).

the increased creep properties after prestraining were due to carbides precipitating on dislocations and offered electron transmission micrographs as proof.

The most important aspect of prestraining on creep may be its effect on creep ductility, as evidenced by the low values found in Table 3. In general, the results presented in this report illustrate that the strength of type 304 stainless steel is improved as a result of exposure to CO<sub>2</sub>. This applies to the test piece exposed to CO<sub>2</sub> both in the absence and presence of stress. The improvement in strength, however, was accompanied by a loss in ductility. The series of tensile tests, which are summarized in Table 4, were run in an effort to evaluate the influence of the carbon distribution on the magnitude of the ductility reduction. They indicated that in general the ductility reduction becomes greater for a given annealing time as the annealing temperature is increased. The rupture ductility can be reduced significantly. For example, average carbon concentrations of 0.2 wt % resulted in room-temperature and 1250°F (677°C) rupture ductilities of 29 and 17%, respectively. Thus far no clear correlation has been shown between the reduction in tensile ductility and the temperature of exposure to CO<sub>2</sub>, but the evaluation has been complicated by the carbon having varied, at different temperatures, in quantity, depth of penetration, and morphology<sup>4</sup> and by the apparent instability in the control samples caused by thermal treatment. Additional testing evaluation is required to advance beyond the status of the generalizations given above.

The creep tests also indicated an influence of CO<sub>2</sub> on the rupture ductility. The data showed (Table 3) that at 1300°F (704°C) the ductility was less in CO<sub>2</sub> than in argon. At 1500 and 1700°F (815 and 927°C) the rupture ductility was greater in CO<sub>2</sub> than in argon. The apparent improvement in ductility is felt to be somewhat false in that most of this strain occurred simultaneously with intergranular cracking of the specimen. Hence the useful elongation was possibly not improved by exposure to CO<sub>2</sub> and actually may have been decreased. The results of

---

<sup>4</sup>R. Stickler and A. Vinckier, "Morphology of Grain-Boundary Carbides and Its Influence on Intergranular Corrosion of 304 Stainless Steel," Trans. Am. Soc. Metals 54, 362 (1961).

tensile tests (Table 4) illustrated the decrease in the ability of a component to deform at relatively high strain rates (0.02 in./in.-min) as a result of exposure to CO<sub>2</sub>. Since such loading rates are often encountered in reactor applications, the absorption of carbon during creep loading is a problem even if the creep ductilities are not significantly influenced.

#### CONCLUSIONS

It was concluded that the creep strength of type 304 stainless steel is greater in CO<sub>2</sub> than in argon, with magnitude increasing with increasing temperature and decreasing stress at a given temperature. The strengthening is primarily due to carburization of the material and is more significant in thin sections of material.

The creep-fracture strains can be enhanced or adversely affected by exposure to CO<sub>2</sub>. This observation must be carefully considered since transient loads superimposed on the steady loads may cause low-ductility fracture. Exposure to CO<sub>2</sub> may reduce the ductility by as much as a factor of 5 under certain conditions.

#### ACKNOWLEDGMENTS

The authors wish to acknowledge the contributions of Metals and Ceramics Division personnel E. Bolling, J. East, V. G. Lane, R. D. Waddell, and C. Dollins for the mechanical property tests, B. McNabb for the C<sup>14</sup> experiments, and M. D. Allen and E. D. Bolling for the metallography. The electron microscopy was under the supervision of J. O. Steigler.

DISTRIBUTION

1. G. M. Adamson
2. S. E. Beall
3. M. Bender
4. R. G. Berggren
5. D. S. Billington
6. E. P. Blizzard
7. E. C. Bohlmann
8. W. E. Browning
9. F. L. Carlsen
10. E. L. Compere
- 11-15. J. H. Coobs
16. W. B. Cottrell
17. J. E. Cunningham
18. J. H. DeVan
19. D. A. Douglas, Jr.
20. R. B. Evans
21. D. E. Ferguson
22. A. P. Fraas
23. J. H. Frye, Jr.
24. A. E. Goldman
25. B. L. Greenstreet
26. W. R. Grimes
27. J. P. Hammond
28. W. O. Harms
- 29-31. M. R. Hill
32. H. W. Hoffman
33. J. A. Lane
34. E. L. Long, Jr.
35. M. I. Lundin
36. H. G. MacPherson
37. W. D. Manly
38. W. R. Martin
39. R. W. McClung
40. H. E. McCoy, Jr.
41. J. G. Morgan
42. N. Ozisik
43. P. Patriarca
44. A. M. Perry
45. M. W. Rosenthal
46. G. Samuels
47. H. W. Savage
48. J. L. Scott
49. O. Sisman
50. G. M. Slaughter
51. E. Storto
52. J. C. Suddath
53. J. A. Swartout
54. D. B. Trauger
55. C. S. Walker
56. J. L. Wantland
57. G. M. Watson
58. M. S. Wechsler
59. J. R. Weir
60. J. C. White
61. J. Zasler
- 62-64. ORNL - Y-12 Technical Library,  
Document Reference Section
- 65-67. Laboratory Records Department
68. Laboratory Records Department,  
ORNL-RC
- 69-71. Central Research Library
72. ORNL Patent Office
73. Division of Research and  
Development, AEC-ORO
- 74-75. David F. Cope, Reactor  
Division, AEC-ORO
- 76-90. Division of Technical  
Information Extension (DTIE)

